Supporting Information

Mazur et al. 10.1073/pnas.1002423107

SI Materials and Methods

Histology and Immunohistology. Specimens were fixed in 4% neutral buffered formaldehyde and embedded in paraffin. Pancreata were sectioned at 3 μm and stained with H&E or used for immunohistochemical studies with antibodies against amylase, insulin (Sigma), CK19 (DSHB), ER, glucagon (Dako), E-cadherin (R&D Systems), PDX1 (gift of C. V. Wright, Vanderbilt University Medical Center, Nashville, TN), HES1 (gift of T. Sudo, Toray Industries Inc., Kamakura, Japan), Myc (Santa Cruz Biotechnology), progesterone receptor (NeoMarkers), and p53 (Novocastra). Staining for mucin content was carried out using a periodic acid–Schiff reaction. X-Gal staining of cryosections (10 μm) was carried out according to standard protocols, and cryosections were counterstained with nuclear fast red. Double-immunofluorescence was performed using Alexa 488 and Alexa 555 (1:1,000; Invitrogen). Nuclei were stained with DAPI. Pictures were taken using an Axiovert 200M fluorescence inverse microscope (Zeiss) equipped with Axiovision software (Zeiss).

Histopathological Evaluation. H&E-stained sections were evaluated by pathologists with expertise in human and mouse PDAC pathology (B.S. and G.K.).

Western Blot Analysis. Protein extracts from tissues or cells were obtained using radioimmunoprecipitation assay buffer, separated on standard SDS/PAGE electrophoresis, transferred to nitrocellulose filters, and incubated with antibodies: β-actin (Sigma), Myc, Notch1 (BD Pharmingen), Notch2 (DSHB), Notch3, Notch4, Delta, Jagged (Santa Cruz Biotechnology), and p53 (Novocastra). Antibody binding was visualized using HRP-labeled secondary antibodies and ECL reagent (Amersham).

Primary Cell Culture and Cell Assays. Cells were maintained in DMEM medium with 10% (vol/vol) FCS, 1% nonessential amino acids, and 1% penicillin/streptomycin. For TGF-β receptor inhibition experiments, the SB431542 inhibitor (Sigma) was used for 48 h at final concentrations of 5 and 10 μM. For migration assays (wound healing), confluent cells were starved with minimal medium (0.5% FCS), scratched with a 20-μL pipette tip to form wounds, and incubated with human recombinant TGF-β1 (R&D Systems) at a final concentration of 5 ng/mL for 48 h. Representative photographs were taken from several high-power fields. Quantification of the wound closure area was performed using Axiovision 4.8 software (Zeiss). Six representative photographs for each time point were analyzed, and the percentage of cell-free area was plotted. For all assays, analysis was performed on low passage number cell lines (fewer than eight passages).

ChIP. Experiments were performed using the EZ-ChIP Kit (Upstate). The following antibodies were used: Notch2 (DSHB), RBP-Jκ (Institute of Immunology Co.), Pol II (Upstate) as a positive control, and IgG as background control. Quantitative PCR was performed on a Lightcycler (Roche) using the primers listed in Table S11. Calculation of average cycle threshold (Ct) and SD for triplicate reactions was performed, and each DNA fraction was normalized to the input to account for chromatin sample preparation differences: $\Delta Ct_{\text{normalized ChIP}} = Ct_{\text{ChIP}} - Ct_{\text{input}} - \text{Log}_2(\text{dilution})$, where "dilution" is input dilution factor = 100. Normalized background was then subtracted using the following equation: $\Delta\Delta Ct = \Delta Ct_{\text{normalized ChIP}} - \Delta Ct_{\text{normalized IgG}}$. The SD was calculated using propagation of error: $SD_{\Delta\Delta Ct} = \sqrt{SD_{ChIP}^2 + SD_{input}^2 + SD_{IgG}^2}$.

Calculation of the relative quantity of amplified sequence (fold enrichment) was carried out according to the following equation: $Q = 2^{-\Delta\Delta Ct}$. Calculation of error for relative quantity was carried out according to the following equation: $Q_{error\pm} = Q \pm 2^{-(\Delta\Delta Ct \pm SD\Delta\Delta Ct)}$.

RT-PCR Assay. RNA was isolated using the Qiagen RNeasy Isolation Kit, followed by cDNA synthesis (SuperScript II; Invitrogen). Real-time PCR was performed with 800-nM primers diluted in a final volume of 20 μL in SYBR Green Reaction Mix (Applied Biosystems). RT-PCR assays were performed as follows: 95 °C for 10 min, followed by 35 cycles of 95 °C for 15 s and 60 °C for 1 min using a LightCycler (Roche). All samples were analyzed in triplicate. Cyclophilin and hypoxanthine guanine phosphoribosyl transferase expression was used for normalization. Primers used are shown in Table S14.

Mutation Analysis of *p53*, *p16/Ink4a*, and *Smad4*. RNA isolated from PDAC cell lines (RNeasy Isolation Kit) was used to generate cDNA (Superscript II) for further analysis essentially as described previously (32[1]). Briefly, amplified (with PfuUltra polymerase; Stratagene) *p53* and *Smad4* gene sequences were cloned into the pCR3.1-TOPO (Invitrogen) plasmid, and *p16/Ink4a*, *p19/Arf* was cloned into pBluescript (Stratagene; restriction sites BamHI and HindIII) and sequenced bidirectionally. Three to eight independent clones were sequenced for each cell line.

Bisulfite Modification and Methylation-Specific PCR Assay. DNA isolated from primary cancer cells was modified by bisulfite treatment (Invitrogen) and PCR-amplified using primers specific for methylated and unmethylated regions of the 5′ UTR of the *p16/Ink4a* locus. Primers used are listed in Table S11.

Luciferase Reporter Assay. A luciferase reporter assay was performed with the following luciferase reporter constructs: Myc-luc, containing three WT *Rbpj* binding sites; Myc-mutA-luc, containing mutated binding site A; Myc-mutAB-luc, including mutated binding sites A and B; and Myc-mutABC-luc, with mutated binding sites A, B, and C. Primary *Kras;N2ko* cancer cells were cultured in a six-well plate and transiently transfected in triplicate with luciferase reporter plasmids, N2IC expression plasmids and pRL-TK (internal control reporter; Promega) using Fugene 6 following the manufacturer's instructions (Roche). Luciferase activity was measured with the dual-luciferase reporter assay system (Promega) 48 h after transfection, with the Renilla luciferase activity serving as an internal control. Results are expressed as a percentage of induction over control (100%).

Gene Chip Analysis and GSEA. Pancreata of two to four mice per genotype were dissected 7 d postnatally. For analysis of PDAC, six different low-passage (fewer than eight passages) cultured cell lines from *Kras* and *Kras;N2ko* PDAC were used. Total RNA was prepared as described above. A total of 1–5 μg of labeled RNA was hybridized to mouse expression gene chip arrays (Mouse Genome 430A 2.0 Array; Affymetrix) according to the manufacturer's protocols. Gene chips were scanned and analyzed using Affymetrix Microarray Suite 5.0 software (MAS 5.0), as described previously (10[2]).

GSEA software was provided by the Broad Institute of the Massachusetts Institute of Technology and Harvard University (http://www.broad.mit.edu/gsea/). We acknowledge the use of the GSEA and GSEA software (60). For both gene sets, we used

the default parameters of the GSEA software package, except for the number of permutations (n = 1,000).

Statistical Analyses. Kaplan–Meier curves were calculated using the survival time for each mouse from all littermate groups (*wt*, *Kras, Kras;N1ko*, and *Kras;N2ko*). The log-rank test was used to test for significant differences between the four groups. For gene expression analysis, the unpaired two-tailed Student's t test was used. $P < 0.05$ was considered significant.

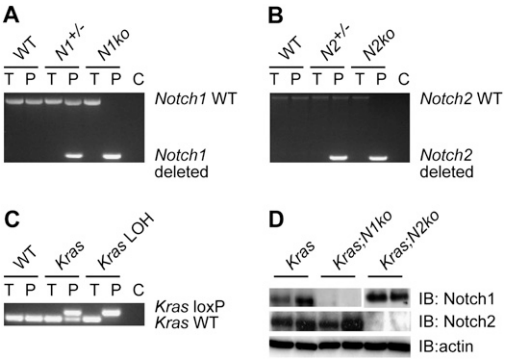

Fig. S1. Targeting endogenous *Kras*^{G12D} expression and *Notch1* and *Notch2* deletion in the pancreas. (*A*) Specific PCR analysis of genomic DNA from pancreata (P) but not tails (T) of *N1ko* mice reveals the expected *Notch1* deletion (C = negative control). (*B*) Specific PCR analysis of genomic DNA from pancreata but not tails of *N2ko* mice reveals the expected *Notch2* deletion. (*C*) Specific PCR analysis of genomic DNA from pancreata but not tails of *Kras* mice reveals the expected stop cassette removal and *Kras*^{G12D} activation. Some pancreata show loss of heterozygosity of the remaining WT *Kras* allele. (*D*) Western blot analysis confirms *Notch1* and *Notch2* ablation in the pancreas. IB, immunoblot.

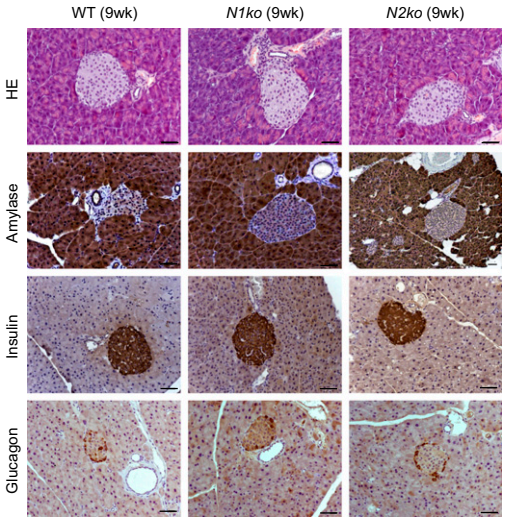

Fig. S2. Architectural and functional integrity of the pancreas in 9-wk-old WT, *N1ko*, and *N2ko* animals and in 12-mo-old *N2ko* animals. Immunohistological detection of amylase, insulin, and glucagon reveals no differences between genotypes.

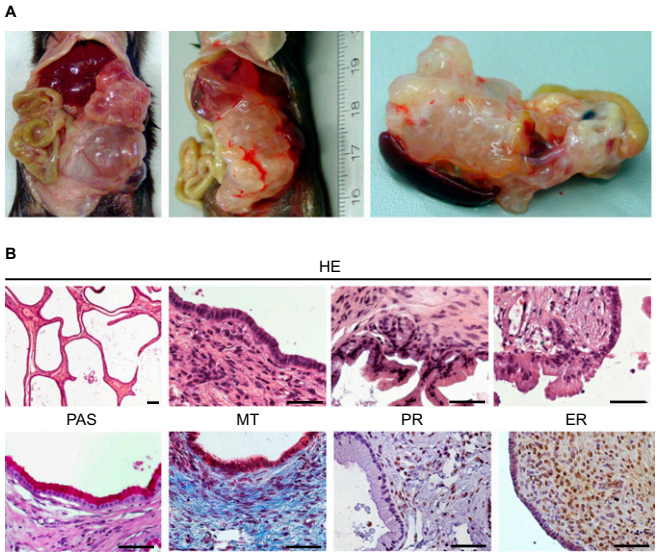

Fig. S3. *Kras;N2ko* mice develop cystic lesions resembling human MCN. (*A*) Typical multilocular cysts develop in the splenic part of the pancreas in aged *Kras;N2ko* mice. (*B*) Cystic lesions are lined by mucinous columnar epithelium positive by PAS staining, focally demonstrating low to moderate levels of dysplasia (*Top Right*). The surrounding highly cellular stromal compartment has abundant collagen deposits, as indicated by Masson–Trichrome staining (MT) and prominent nuclear expression of progesterone receptor (PR) and/or ER. (Scale bar: 50 μm.)

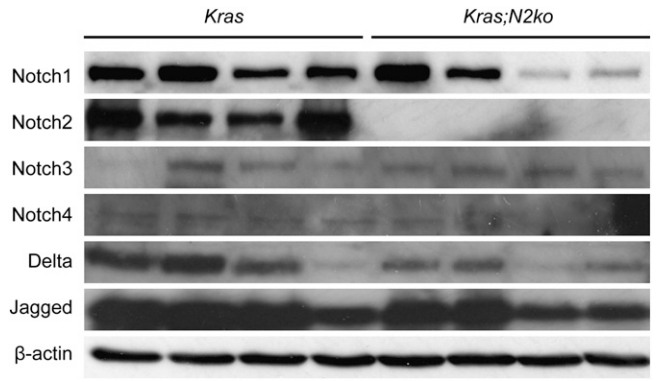

Fig. S4. Notch receptor and ligand protein expression in *Kras* and *Kras;N2ko* primary tumor cells.

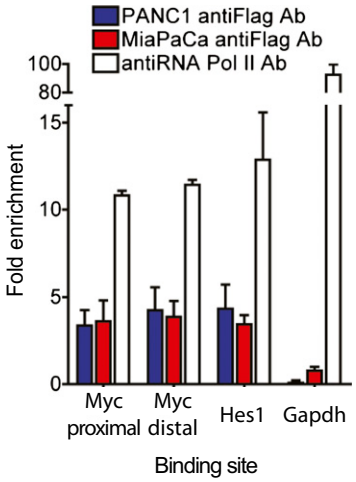

Fig. S5. ChIP was performed in human pancreatic cancer cell lines Panc1 and MiaPaCa2. Cells were transiently transfected with pCMV-Notch2-IC-Flag construct, and anti-Flag antibody was used to analyze whether Myc is a direct transcriptional target of Notch2. Quantitative PCR indicates that Notch2 binds to regions proximal and distal in the human *Myc* promoter (corresponding to Myc site A and B + C in the murine promoter, respectively), comparable to a binding site of the *Hes1* promoter. A nonbinding *Gapdh* promoter region and RNA Polymerase III binding serve as controls.

Table S1. Immunohistochemical analyses of PanINs, MCN, invasive PDA, and metastases in *Kras* mice

	PanIN				MCN				Tumor				Metastases			
Marker	N	F	P	I	N	F	P	I	N	F	P	I	N	F	P	I
TP53	5/9	+++	++	++	2/3	++	++	+	4/9	++	++	+	1/3	+++	+++	++
PDX1	9/9	++	++	+	3/3	+++	+++	++	9/9	++	++	+	2/3	+++	+++	+++
CK19	9/9	+++	+++	++	3/3	+++	+++	+++	9/9	+++	+++	++	3/3	+++	+++	+++
E-CAD	9/9	+++	+++	++	3/3	+++	+++	+++	9/9	+++	+++	++	3/3	+++	+++	+++
HES1	9/9	+++	+++	+	3/3	+++	+++	+	9/9	+++	++	+	3/3	+++	++	+
MYC	8/8	+++	+++	+++	2/2	++	++	+	8/8	+++	+++	+++	3/3	+++	+++	+++

F, frequency of lesions (or discrete regions of tumor) that scored positive per tissue sample (+, <10%; ++, 10–50%; +++, >50%); I, intensity of expression per positive cell (+, weak; ++, moderate; +++, strong); N; number of tissue samples with positive lesions over total evaluated; P, percentage of cells within a specified lesion that were positive (+ <10%; ++, 10–50%; +++, >50%).

Table S2. Immunohistochemical analyses of PanINs, MCN, invasive PDA, and metastases in *Kras;N1ko* mice

	PanIN				MCN				Tumor				Metastases			
Marker	N	F	P	I	N	F	P	I	N	F	P	I	N	F	P	I
TP53	6/9	++	+	+	2/4	++	+	+	0/7	n/a	n/a	n/a	n/d			
PDX1	5/8	++	++	+	4/4	++	++	+	2/8	++	++	+	n/d			
CK19	6/6	+++	+++	++	3/3	+++	+++	+++	6/6	+++	+++	++	n/d			
E-CAD	6/6	+++	+++	++	3/3	+++	+++	+++	6/6	+++	+++	++	n/d			
HES1	9/9	+++	+++	+	4/4	+++	+++	+	9/9	++	++	+	n/d			
MYC	3/3	+++	+++	+++	n/d				3/3	+++	+++	+++	n/d			

F, frequency of lesions (or discrete regions of tumor) that scored positive per tissue sample (+, <10%; ++, 10–50%; +++, >50%); I, intensity of expression per positive cell (+, weak; ++, moderate; +++, strong); N; number of tissue samples with positive lesions over total evaluated; n/a, not applicable; n/d, not determined; P, percentage of cells within a specified lesion that were positive (+ <10%; ++, 10–50%; +++, >50%).

Table S3. Immunohistochemical analyses of PanINs, MCN, invasive PDA, and metastases in *Kras;N2ko* mice

	PanIN				MCN				Tumor				Metastases			
Marker	N	F	P	I	N	F	P	I	N	F	P	I	N	F	P	I
TP53	8/10	++	+	+	5/7	++	++	+	6/10	+	+	+	0/3	n/a	n/a	n/a
PDX1	10/10	+++	+++	+++	7/7	+++	+++	+++	10/10	+++	+++	++	3/3	+++	+++	++
CK19	10/10	+++	+++	+++	7/7	+++	+++	+++	5/10	++	+	+	1/3	Z	++	+
E-CAD	10/10	+++	+++	+++	7/7	+++	+++	+++	5/10	++	+	+	1/3	Z	++	+
HES1	10/10	+++	+	+	7/7	++	+	+	10/10	+++	++	+	3/3	+++	++	+
MYC	8/8	++	++	+	5/5	++	++	+	8/8	++	++	+	2/2	++	+	+

F, frequency of lesions (or discrete regions of tumor) that scored positive per tissue sample (+, <10%; ++, 10–50%; +++, >50%); I, intensity of expression per positive cell (+, weak; ++, moderate; +++, strong); N; number of tissue samples with positive lesions over total evaluated; n/a, not applicable; P, percentage of cells within a specified lesion that were positive (+ <10%; ++, 10–50%; +++, >50%); Z, presence of stochastic heterogeneity.

Table S4. Clinical spectrum of disease in *Kras* mice

				Histology						
Identification no.	Age, d	MCN	PDAC	>50%	<50%	Liver	Lung	Ascites	Cachexia	Other
2190	467	N	Y	G	U, S	Y^{M}	Y^{M}	Y	Y	
4874	358	N	N			N	N	N	N	Postmortem
5630	538	N	N			N	N	N	N	FAP
9801	300	N	Y	G		Y^{M}	Y^{M}	Y^{B}	Y	LN^{M}
9425	209	N	N			N	N	N	N	F
9907	444	N	Y	G		Y^{M}	N	N	N	
10265	603	N	Y	G		Y^{M}	Y^{M}	N	N	F
10266	425	N	Y	G		Y^{M}				SM
10259	269	N	N							
10526	523	Y	Y	U		Y^{M}	N	N	N	
11752	347	N	N			N	N	N	Y	
14128	482	Y	Y	G		Y^{M}	N	Y^{B}	N	AD, LN^{M}, A^{m}, SM
17027	239	N	Y	G		Y^{M}	Y^{M}	N	N	
17165	576	N	N					Y		D^{inv}
17395	512	N	N							F
17654	335	N	N			N	N	N	N	
19476	630	N	N			N	N	N	N	F, FAP
20283	489	N	Y	G	U	N	N			Steatosis of liver
50709	635	Y	Y	G	U					F
52231	427	N	N			N	N	N	N	F
54474	311	N	N							
510042	569	N	Y	G		Y^{M}	Y^{M}	Y^{B}		SM
510046	330	N	N			N	N	Y^{B}	N	Hemorrhage, Panc necrosis
510242	421	N	Y	G		N	N	N	N	
510256	293	N	Y	U	G	N	N	N	N	LN^{M}, SM
610020	288	N	Y	G		Y^{M}	Y^{M}	N	N	F
Total		3/26	14/26			10/26	6/26	5/26	3/26	
%		12%	54%			38%	23%	19%	12%	

A, adrenal gland; AD, abdominal distention; ^{B}, bloody ascites; D^{inv}, duodenum invasion; F, fibrosis; FAP, fat atrophy of the pancreas; G, glandular; LN, lymph node; ^{M}, macrometastasis; ^{m}, micrometastasis; N, no; Panc, pancreas; S, sarcomatoid; SM, splenomegaly (spleen >20 mm); U, undifferentiated; Y, yes.

Table S5. Clinical spectrum of disease in *Kras;N1ko* mice

Identification no.	Age, d	MCN	PDAC	Histology >50%	Histology <50%	Liver	Lung	Ascites	Cachexia	Other
818	594	N	N			N	N	N	Y	SM, lymphoma
1015	198	N	Y	S		N	N	N	Y	A^{M}, D^{inv}, liver necrosis
1016	226	N	N			N	N	N	N	FAP
4894	337	Y	N			N	N	Y^{B}	Y	Panc necrosis
5051	278	N	N			N	N	N	Y	Respiration insufficiency
5306	357	N	Y	G		N	N	N	Y	FAP, spleen necrosis
6340	563	N	N			N	N	N	N	FAP
6344	325	N	Y	G	U, S	Y^{M}	Y^{M}	Y	Y	LN^{M}
6364	300	N	Y	U	S	Y^{M}	Y^{M}	N	N	
6361	549	Y	Y	S	G	N	N	N	N	LN^{M}, FAP
6367	248	N	Y	G		Y	N	N	Y	SM, bronchitis
7289	336	N	N			N	N	N	Y	Icterus, liver necrosis, lung thromboembolism
9372	482	N	N			N	N	N	Y	Panc granulomatous inflammation, hepatitis
9382	566	Y	Y	G	S	N	N	N	N	IPMN, FAP
9854	197	N	N			N	N	N	N	FAP
9857	659	N	N			N	N	N	N	FAP
11741	298	N	N			N	N	N	Y	
15625	203	Y	Y	G	S	N	N	N	N	AD, SM
17906	374	N	N			N	N	N	N	FAP
17908	285	N	N			N	N	N	N	
50825	199	Y	Y			N	N	Y^{B}	N	Liver necrosis, bronchitis
52138	400	N	N			N	N	N	N	
54665	419	N	N			N	N	N	N	Hemorrhage
Total		6/23	9/23			3/23	2/23	2/24	9/23	
%		26%	39%			13%	9%	9%	39%	

A, adrenal gland; AD, abdominal distention; D^{inv}, duodenum invasion; FAP, fat atrophy of the pancreas; G, glandular; IPMN, intraductal papillary mucinous neoplasm; LN, lymph node; ^{M}, macrometastasis; N, no; Panc, pancreas; S, sarcomatoid; SM, splenomegaly (spleen >20 mm); U, undifferentiated; Y, yes.

Table S6. Clinical spectrum of disease in *Kras;N2ko* mice

Identification no.	Age, d	MCN	PDAC	Histology >50%	Histology <50%	Liver	Lung	Ascites	Cachexia	Other
998	438	Y	N			N	N	N	N	AD
999	438	Y	N			N	N	N	N	AD
1002	478	Y	N			N	N	N	Y	
1003	474	Y	N			N	N	N	Y	AD, D^{inv}
1006	464	Y	Y	S		Y^{M}	N	Y	Y	AD, LN^{m}
1009	669	Y	Y	S	U^{G3}	Y^{M}	Y^{M}	N	N	LN^{m}, D^{inv}
1013	580	Y	Y	S		Y^{M}	Y^{m}	N	N	AD
1014	457	Y	N			N	N	N	Y	
3113	567	Y	Y	S	U^{G3}	Y^{M}	Y^{m}	N	N	AD
5111	648	Y	N			N	N	N	N	E, pneumonia
5112	558	Y	Y	S		Y^{M}	N	Y^{B}	N	D^{inv}, LN^{M}
5114	717	Y	N			N	N	N	N	Blind
10894	608	N	Y	S		Y^{M}	N	N	N	AD, D^{inv}
14054	557	Y	N			N	N	N	N	D^{inv}
17656	335	N	Y	G	U^{G3}	Y^{M}	Y^{M}	N	N	LN^{m}, A^{M}
17693	461	Y	Y	S	G	Y^{M}	N	N	N	Sudden death
17915	556	Y	N			N	N	N	N	Panc insufficiency
17916	556	Y	N	*	*	*	*	N	Y	AD, post mortem
50753	521	Y	Y	G		N	N	N	Y	
54658	393	Y	Y	G	U^{G3}	Y^{M}	N	N	N	Panc necosis
55079	396	N	Y	S		Y^{M}	Y^{m}	Y^{B}	N	D^{inv}
Total		18/21	11/21			10/20	5/20	3/21	6/21	
%		86%	52%			50%	25%	14%	29%	

A, adrenal gland; AD, abdominal distention; D^{inv}, duodenum invasion; E, edema; G, glandular; LN, lymph node; ^{M}, macrometastasis; ^{m}, micrometastasis; N, no; Panc, pancreas; S, sarcomatoid; U, undifferentiated; Y, yes.
*Not evaluable.

Table S7. Characteristics of the stromal compartments of *Kras, Kras;N1ko, and Kras;N2ko* mice

	Kras			*Kras;N1ko*			*Kras;N2ko*			*Myc ko*		
Marker	N	P	I	N	P	I	N	P	I	N	P	I
PR	8/15	+	+	4/11	+	+	17/18	++	++	2/2	++	++
ER	0/15	–	–	1/11	+	+	9/18	+	+	2/2	+	+

I, intensity of expression per positive cell (+, weak; ++, moderate); N, number of tissue samples with positive stroma over total evaluated; P, percentage of cells within a stroma that were positive (+, <10%; ++, 10–50%; +++, >50%); PR, progesterone receptor.

Table S8. Molecular profiles of *Kras* primary pancreatic cancer cell lines

	p16				p19			p53			Smad4	
Identification no.	DNA	mRNA	Protein	Promoter	DNA	Protein	Promoter	DNA	mRNA	Protein	mRNA	Protein
2190	del	–	–	n/a	del	–	n/a	mut	+	+	+	+
9801	del	–	–	n/a	del	–	n/a	wt	+	–	+	+
17027	mut	+	–	n/a	n/d	–	n/d	wt	+	–	+	+
10265	n/a	n/a	–	M	n/a	–	M	n/a	–	–	+	+
13092	n/a	n/a	–	M	n/a	–	M	mut	+	–	+	+

del, deletion; M, methylated; mut, mutation; n/a, not applicable; n/d, not determined; wt, wild type.

Table S9. Molecular profiles of *Kras;N2ko* primary pancreatic cancer cell lines

	p16				p19			p53			Smad4	
ID	DNA	mRNA	Protein	Promoter	DNA	Protein	Promoter	DNA	mRNA	Protein	mRNA	Protein
1006	del	–	–	n/a	del	–	n/a	wt	+	–	+	+
1009	mut	+	–	U	mut	–	n/a	wt	+	–	+	+
1013	wt	+	–	M	n/a	–	M	wt	+	–	+	+
3113	del	–	–	n/a	del	–	n/a	wt	+	–	+	+
5112	n/a	n/a	–	M	n/a	–	M	wt	+	–	+	+

del, deletion; M, methylated; mut, mutation; n/a, not applicable; U, unmethylated; wt, wild type.

Table S10. Top 20 and selected TGF-β GSEA signature analysis of *Kras;N2ko vs. Kras* in 7-d-old pancreata

TGF-β signature	No.	Name	Size	ES	NES	NOM *P* value	FDR Q value	FWER *P* value	Rank at maximum
	1	VEGF_MMMEC_6HRS_UP	63	−0.73973954	−2.7084892	0	0	0	2449
I	2	TGFBETA_ALL_UP	122	−0.6643366	−2.6893036	0	0	0	3697
II	3	TGFBETA_EARLY_UP	67	−0.7087745	−2.6222773	0	0	0	2828
	4	HTERT_DN	88	−0.67262614	−2.61393	0	0	0	2203
	5	CROONQUIST_RAS_STROMA_DN	35	−0.7753971	−2.526193	0	0	0	1506
	6	CROONQUIST_IL6_STROMA_UP	62	−0.6876837	−2.5074594	0	0	0	2646
	7	VEGF_MMMEC_12HRS_UP	40	−0.7396944	−2.4997904	0	0	0	2703
	8	CMV_ALL_DN	165	−0.5892903	−2.4887757	0	0	0	3137
	9	CMV_24HRS_DN	115	−0.60143775	−2.4474874	0	0	0	3137
	10	ADIP_VS_PREADIP_DN	61	−0.6479043	−2.3746915	0	0	0	2203
	11	SANA_TNFA_ENDOTHELIAL_DN	129	−0.5758857	−2.3746207	0	0	0	3153
	12	CORDERO_KRAS_KD_VS_CONTROL_UP	124	−0.5773957	−2.358846	0	0	0	3808
	13	VEGF_MMMEC_ALL_UP	134	−0.5670125	−2.3364904	0	0	0	3170
	14	JNK_DN	53	−0.6561161	−2.336097	0	0	0	1504
	15	EMT_UP	89	−0.595401	−2.3324068	0	0	0	1812
	16	ADIP_VS_FIBRO_DN	45	−0.6774173	−2.3317726	0	0	0	1704
	17	PASSERINI_EM	52	−0.65962523	−2.3163188	0	0	0	1188
	18	NI2_MOUSE_UP	68	−0.62407684	−2.3120317	0	0	0	2273
	19	CMV_HCMV_6HRS_DN	86	−0.5928433	−2.2827766	0	0	0	2639
III	20	TGFBETA_LATE_UP	55	−0.6278115	−2.2798045	0	0	0	3697
IV	27	TGFBETA_C1_UP	26	−0.71738595	−2.1937995	0	0	0	3125
V	50	TGFBETA_C2_UP	21	−0.7205094	−2.0788	0	1.08E-04	0.004	2481
VI	59	TGFBETA_C3_UP	20	−0.71528685	−1.978819	0	8.68E-04	0.038	2828
VII	103	TGF_BETA_SIGNALING_PATHWAY	73	−0.47657073	−1.8012985	0	0.005866292	0.356	3045
VIII	210	TGFBETA_C5_UP	28	−0.50880885	−1.5387949	0.03522505	0.04333228	1	3507

NOM, nominal; FDR, false discovery rate; FWER, familywise-error rate.

Table S11. Top 20 and selected TGF-β GSEA-signature analysis of *Kras;N2ko vs. Kras* in primary cancer cells

TGF-β signature	No.	Name	Size	ES	NES	NOM *P* value	FDR *Q* value	FWER *P* value	Rank at maximum
	1	BRCA1_SW480_DN	25	0.57281667	1.6047903	0.016260162	1	0.941	4867
	2	STANELLE_E2F1_UP	37	0.5446293	1.5969661	0.029411765	1	0.959	4800
	3	ROSS_MLL_FUSION	92	0.51262605	1.5786657	0.013779528	1	0.976	3624
	4	DFOSB_BRAIN_2WKS_UP	70	0.4554071	1.5774709	0.02258727	1	0.977	3462
	5	BECKER_ESTROGEN_RESPONSIVE_SUBSET_2	16	0.7206843	1.5664608	0.062248997	1	0.981	3974
	6	PITUITARY_FETAL_UP	20	0.5904766	1.5654356	0.020661157	1	0.981	2282
I	7	TGFBETA_C3_UP	22	0.7693509	1.557574	0.012048192	1	0.983	4837
	8	PASSERINI_EM	52	0.5384598	1.5406632	0.041420117	1	0.991	4491
	9	HIPPOCAMPUS_DEVELOPMENT_POSTNATAL	93	0.40995428	1.5284934	0.056092843	1	0.992	4648
	10	MATRIX_METALLOPROTEINASES	40	0.60774666	1.5278989	0.025590552	1	0.992	5098
	11	BCNU_GLIOMA_MGMT_48HRS_DN	236	0.38457447	1.5273094	0	1	0.992	3432
	12	CREB_BRAIN_2WKS_UP	50	0.5023513	1.5242647	0.02892562	1	0.992	5003
	13	BCNU_GLIOMA_NOMGMT_48HRS_DN	39	0.53599626	1.5200945	0.0480167	1	0.993	5916
	14	CMV_24HRS_DN	120	0.5040459	1.5176041	0.021568628	1	0.994	5554
	15	P21_ANY_UP	21	0.54496384	1.5051401	0.038934425	1	1	1451
	16	BRENTANI_CYTOSKELETON	36	0.49675605	1.494601	0.04733728	1	1	3546
	17	TSA_HEPATOMA_CANCER_UP	63	0.5483822	1.4906943	0.014141414	1	1	5229
	18	HOGERKORP_ANTI_CD44_DN	17	0.619508	1.4869046	0.02739726	1	1	3159
II	19	TGFBETA_C2_UP	23	0.6331687	1.4660585	0.058091287	1	1	3449
	20	AGED_MOUSE_CEREBELLUM_UP	87	0.40096402	1.4480395	0.019417476	1	1	3658
III	49	TGFBETA_C5_UP	29	0.5311824	1.3228422	0.13373253	1	1	2431
IV	60	TGFBETA_ALL_UP	131	0.44838282	1.3071258	0.13582677	1	1	3449
V	63	TGFBETA_EARLY_UP	74	0.46519884	1.3036715	0.14741036	1	1	3449
VI	99	TGFBETA_LATE_UP	57	0.4385211	1.2246829	0.19379845	0.9441126	1	2431
VII	300	TGF_BETA_SIGNALING_PATHWAY	77	0.27689424	0.90238446	0.6062992	0.95473385	1	5197

Table S12. Top 20 and selected Myc GSEA-signature analysis of *Kras vs. Kras;N2ko* in 7-day pancreata

Myc signature	No.	Name	Size	ES	NES	NOM *P* value	FDR *Q* value	FWER *P* value	Rank at maximum
	1	ELECTRON_TRANSPORT_CHAIN	158	0.5342571	2.300599	0	0	0	4326
	2	TRNA_SYNTHETASES	27	0.7419937	2.2859864	0	0	0	4208
I	3	COLLER_MYC_UP	32	0.6781227	2.216999	0	3.84E-04	0.002	2778
	4	IDX_TSA_UP_CLUSTER5	145	0.50770676	2.158931	0	8.76E-04	0.006	4059
	5	LEE_E2F1_DN	78	0.53141326	2.0727038	0	0.001649699	0.014	3441
	6	LEE_DENA_DN	91	0.5156025	2.0725226	0	0.001374749	0.014	1955
	7	IDX_TSA_UP_CLUSTER6	257	0.4502082	2.0651782	0	0.001441618	0.017	4497
	8	WELCSH_BRCA_DN	23	0.67598593	2.0217664	0.001945525	0.002307167	0.03	2810
	9	CANTHARIDIN_DN	78	0.5077346	1.9852358	0	0.003184209	0.047	5920
II	10	SCHUMACHER_MYC_UP	87	0.48875225	1.9593258	0	0.004319648	0.07	3945
III	11	ZELLER_MYC_UP	43	0.5399944	1.8503262	0	0.015880471	0.262	2889
	12	CAMPTOTHECIN_PROBCELL_UP	34	0.56002825	1.8316183	0	0.0168502	0.294	520
	13	WELCH_GATA1	31	0.5687488	1.8138825	0.004149378	0.018689869	0.337	3743
	14	LIZUKA_G2_GR_G3	49	0.4995041	1.8052945	0.004115226	0.019245178	0.368	2443
	15	FETAL_LIVER_VS_ADULT_LIVER_GNF2	82	0.46067837	1.7911378	0	0.021657487	0.422	3410
	16	HSC_INTERMEDIATEPROGENITORS_FETAL	193	0.39740488	1.7571981	0	0.029404327	0.542	4533
	17	TGZ_ADIP_UP	31	0.5390484	1.7285321	0	0.0372291	0.66	3874
	18	CHAUVIN_ANDROGEN_REGULATED_GENES	53	0.47623584	1.7251784	0	0.036329415	0.672	3578
	19	TARTE_PC	121	0.41285878	1.722183	0	0.035080407	0.68	2706
	20	FATTY_ACID_METABOLISM	86	0.43455413	1.7186521	0.00212766	0.03449751	0.695	3522
IV	23	LEE_MYC_E2F1_DN	70	0.4449714	1.6893218	0	0.040535	0.797	1955
V	46	LEE_MYC_TGFA_UP	86	0.38082185	1.4974045	0.01594533	0.10934354	1	1104
VI	50	LEE_MYC_TGFA_DN	74	0.38602623	1.4770054	0.027777778	0.11692726	1	3386
VII	55	LEE_MYC_DN	70	0.3735229	1.4269519	0.017699115	0.15354133	1	2455
VIII	69	MYC_TARGETS	71	0.34512275	1.335033	0.042600896	0.2337143	1	2254
IX	137	MENSSEN_MYC_UP	56	0.29244816	1.0630429	0.3197556	0.5902829	1	2950

Table S13. Top 20 and selected Myc GSEA-signature analysis of *Kras vs. Kras;N2ko* in primary cancer cells

Myc signature	No.	Name	Size	ES	NES	NOM *P* value	FDR *Q* value	FWER *P* value	Rank at maximum
	1	RADIATION_SENSITIVITY	41	−0.5413243	−1.7699555	0	0.6791079	0.406	345
	2	LIZUKA_L0_GR_L1	20	−0.63693947	−1.6705452	0.01996008	1	0.81	2738
	3	HIPPOCAMPUS_DEVELOPMENT_PRENATAL	58	−0.52234524	−1.6371815	0.013461539	1	0.9	1985
	4	FERRANDO_LYL1_NEIGHBORS	23	−0.5858673	−1.6352273	0.033264033	1	0.904	68
	5	SMITH_HTERT_UP	155	−0.45070013	−1.6220243	0.00591716	0.95484215	0.919	4327
	6	BYSTRYKH_HSC_BRAIN_CIS_GLOCUS	130	−0.45005926	−1.6199737	0.003752345	0.817574	0.919	4532
	7	CMV_HCMV_TIMECOURSE_18HRS_UP	101	−0.47429216	−1.6039898	0	0.81278753	0.951	5032
	8	YAMA_RECURRENT_HCC_UP	26	−0.6083519	−1.5693748	0.024	1	0.972	68
I	9	COLLER_MYC_UP	33	−0.64743054	−1.5649265	0.030425964	0.93578124	0.974	4101
	10	DAC_FIBRO_UP	32	−0.6267182	−1.5453129	0.02892562	1	0.98	434
II	11	ZELLER_MYC_UP	46	−0.54964083	−1.5182744	0.046511628	1	0.989	1941
	12	BYSTRYKH_HSC_CIS_GLOCUS	229	−0.36202464	−1.5155611	0	1	0.989	4357
III	13	MYC_TARGETS	74	−0.50701964	−1.508564	0.07170542	1	0.991	4478
	14	UVC_HIGH_D2_DN	57	−0.45448267	−1.4786458	0.041501977	1	0.998	3948
	15	STEMCELL_COMMON_UP	315	−0.4237171	−1.4669318	0.05511811	1	0.998	6368
	16	HDACI_COLON_SUL24HRS_UP	105	−0.43819037	−1.4586589	0.050403226	1	0.998	5993
	17	HDACI_COLON_CLUSTER10	50	−0.41208372	−1.4579145	0.017307693	1	0.998	4566
	18	HDACI_COLON_CLUSTER5	37	−0.44846	−1.4569557	0.028985508	1	0.998	3738
	19	VENTRICLES_UP	307	−0.3362042	−1.4472296	0.044624746	1	0.998	4557
	20	UVB_NHEK2_DN	160	−0.32544827	−1.4116431	0.020449897	1	1	5077
IV	25	SCHUMACHER_MYC_UP	92	−0.43308792	−1.3953692	0.12645914	1	1	3422
V	127	LEE_MYC_UP	95	−0.28379893	−1.1302445	0.29492188	0.9526402	1	3889
VI	321	LEE_MYC_TGFA_UP	88	−0.24205469	−0.7627981	0.7643312	1	1	4431
VII	342	FERNANDEZ_MYC_TARGETS	280	−0.17656198	−0.727881	0.91581106	1	1	4997
VIII	361	MENSSEN_MYC_UP	57	−0.23652063	−0.6912166	0.8199234	1	1	7119

Table S14. PCR primers (5′–3′) used

Name	Forward	Reverse
qRT-PCR-Notch1	TGTGCTTTCACACTGGCACAG	CCACTTAGAAGGAATTCCACC
qRT-PCR-Notch2	CCCAGAACCAATCAGGTTAGC	GCCGAGACTCTAGCAATCACAA
qRT-PCR-Notch3	TGGCTCTACTGCACTGATCCTG	CAAGCTCATCCACTGCATTGAC
qRT-PCR-Notch4	GGACTACACCTTTGATGCTGGC	TTCCCCTTTTATCCCTGGCTC
qRT-PCR-Hes1	CGGTGTTAACGCCCTCACA	CGGCTTCAGCGAGTGCAT
qRT-PCR-Ecad	CGTCCTGCCAATCCTGATGAA	ACCACTGCCCTCGTAATCGAA
qRT-PCR-Vim	CATCTCTGGTCTCACCGTCTT	GCCTCTGCCAACCTTTTCTT
qRT-PCR-TGFb1	GTACAGCAAGGTCCTTGCCCT	TAGTAGACGATGGGCAGTGGC
qRT-PCR-Twist	CGGGTCATGGCTAACGTG	CAGCTTGCCATCTTGGAGTC
qRT-PCR-Myc	AAGCTGGTCTCGGAGAA	GGTTTGCCTCTTCTCCAC
qRT-PCR-Cyp	ATGGTCAACCCCACCGTGT	TTCTGCTGTCTTTGGAACTTTGTC
ChIP-Myc SiteA	AAGAGAAAATGGTCGGGCGCGCAGTT	GCGGGGATTAGCCAGAGAATCTCTCT
ChIP-Myc SiteB	AACGTTACTTTGATCTGATCAGGGCC	AAGGCGCTAGACGCGAGAATATGCC
ChIP-Myc SiteC	AACGGAAGCATACACACACAATTCG	CGTTTTCTGAGTACAAAGACCAACCA
ChIP-Hes1	AGACCTTGTGCCTAGCGGCCAATG	AGGGCTACTTAGTGATCGGTAGCAC
ChIP-Cdc2a	GCATTTGAATTGTGTTAGTCTTGGAGGG	TCCGCCAATCCGATTGCACGTAGAC
ChIP-hMyc-proximal	CCCGAGACTGTTGCAAACC	ACTGAGTCCCCCAATTTGCT
ChIP-hMyc-distal	AGAGGGAGCAAAAGAAAATGG	AGAGGGAGCAAAAGAAAATGG
ChIP-hHes1	CCAAATCCAAACGAGGAATTT	GGACGGGTGTAAGAATGTGAG
ChIP-hGAPDH	TACTAGCGGTTTTACGGGCG	TCGAACAGGAGGAGCAGAGAGCGA
p16-methylated	CGATTGGGCGGGTATTGAATTTTCGC	CACGTCATACACACGACCCTAAACCG
p16-unmethylated	GTGATTGGGTGGGTATTGAATTTTTGTG	CACACATCATACACACAACCCTAAACCA
p19-methylated	AATCGAAAATAAATAACGTTTTCGC	TTTAAACCCTTAACGATACGTACG
p19-unmethylated	AAATTGAAAATAAATAATGTTTTTGG	TTAAACCCTTAACAATACACTACAT